Optimisation of Synthesis Parameters for Co-Mo/MgO Catalyst Yield in MWCNTs Production

A. S. Buhari[1], A. S. Abdulrahman[2], S. A. Lawal[1], A. S. Abdulkareem[3], R. A. Muriana[2], O. T. Jimoh[4], H. K. Ibrahim[1,5*]

[1]Department of Mechanical Engineering, Federal University of Technology Minna, Nigeria.
[2]Department of Material and Metallurgical Engineering, Federal University of Technology Minna, Nigeria.
[3]Department of Chemical Engineering, Federal University of Technology Minna, Nigeria.
[4]Department of Chemistry, Federal University of Technology Minna, Nigeria.
[5]Department of Mechanical Engineering, University of Ilorin, Ilorin Nigeria

ABSTRACT: This study examined the impact of synthesis parameter on Cobalt-Molybdenum supported with magnesium oxide (Co-Mo/MgO) catalyst yield in production of multiwall carbon nanotube (MWCNT). Wet impregnation was used to synthesis the Co-Mo/MgO bimetallic catalyst, while a catalytic chemical vapour deposition reactor (CCVD) was used for the synthesis of carbon nanotubes (CNTs). Factorial and central composite design techniques were used to optimise the catalyst and multi-wall carbon nanotubes (MWCNTs). Thermogravimetric analysis/ Differential thermal analysis (TGA/DTA), selected area (electron) diffraction (SAED), X-Ray diffraction analysis (XRD), and Brunauer–Emmett–Teller (BET) were used to characterise the catalyst and MWCNTs that were produced. The Co-Mo/MgO catalyst had an optimal yield of 93.22%, 247.30 m^2/g of specific surface area at 120 ^oC drying temperature, 16 g of mass support, and a 10-hour drying time. The maximum catalyst yield of 40.62% was obtained at calcination temperature of 500 ^oC and a holding period of 2 hours. The catalyst with the highest degradation temperature of 398.21 ^oC was observed at 600 ^oC, when calcined for 4 hours. It was discovered that the surface area of Co-Mo/MgO catalyst from the BET analysis under ideal conditions varied depending on the holding time. The XRD and SAED revealed the growth of CNTs of concentric graphene pattern with the Co-Mo/MgO catalyst.

KEYWORDS: MWCNTs, Thermal Stability, Catalyst, Optimisation, Yield

[Received Oct. 12, 2022; Revised Jan 13, 2023; Accepted April 4, 2023] Print ISSN: 0189-9546 | Online ISSN: 2437-2110

I. INTRODUCTION

The development of nanotechnology was enhanced or fast-tracked by the synthesis and use of carbon nanotubes (CNTs). This is because CNTs have unique physical and chemical characteristics and provide solutions to several technological and environmental issues (Betar *et al*., 2021). Methods that have been used to produce CNTs include arc-discharge, catalytic chemical vapor deposition (CCVD) and laser ablation (Li *et al*., 2020; Brachetti-Sibaja *et al*., 2021; Hashempour *et al*., 2014; Tijani *et al*., 2020 & Thapa *et al*., 2018). Among the methods, CCVD was widely acknowledged for production of CNTs on a commercial scale due to low cost, and large yield as opposed to the other methods (Kim and Lee, 2018). Elements of Group eight and first periodic row of periodic table are typically transition metals (Fe, Co, Ni and their alloys) and are used frequently in the synthesis of catalysts, alone or with the addition of molybdenum (Mo) (Awadallah *et al*., 2014). Adjusting the catalytic support and synthesis parameters, which enables the changing of the size and distribution of catalytic metals, is necessary to maximise the catalyst's effectiveness for the growth and quality of CNTs of various morphologies (Thapa *et al*., 2018; Lobiak *et al*., 2020). The use of MgO as one of the catalytic support materials can result in the maximum yield for the synthesis of CNTs. Processes used to produce support catalysts include combustion, impregnation, precipitation, and sol-gel. (Lobiak *et al*., 2020).

Recently, it has been reported that bimetallic and polymetallic catalysts with various supports are superior to monometallic catalysts for the production of CNTs (Li *et al*., 2020). The Fe/MgO, Fe/Al2O3, Co/MgO, Ni-Cu/MgO, FeMo/MgO, Ni/Mo/MgO and Co-Ni/SiO2, Fe–Co/MgO and Co-Mo/MgO catalysts have been used to synthesised different types of CNTs ranging from single-walled carbon nanotubes (SWNT) double-walled carbon nanotubes (DWNT) and multi-walled carbon nanotubes (MWNT) (Li *et al*., 2020; Ryu *et al*., 2008; Kim and Lee 2018; Buhari *et al*., 2019; Betar *et al*., 2021). The majority of these catalysts were used in earlier research primarily to increase yield and make CNTs more super-hydrophobic while altering the catalyst's composition, combination, and manufacturing method (Kim and Lee 2018). However, it is crucial to optimise the reaction gas flow rate, temperature, and duration to produce CNTs of higher yield and good quality (Li *et al*., 2020). Meanwhile, Ryu et al., (2008) obtained maximum yield using 50% Co (MgO: 50%) catalyst at 600oC for synthesising and optimising MWCNTs on Co-Ni/MgO catalyst using Thermal CVD. The optimisation of the reaction's time, temperature, and H2 gas flow rate revealed that the removal of Ni makes Co a more efficient catalyst. Some researches claimed that adding molybdenum to the Co/MgO catalyst increased the yield and improved the quality of CNTs.

*Corresponding author: ibrahim.kh@unilorin.edu.ng

doi: http://dx.doi.org/10.4314/njtd.v18i4.1409

(Li *et al*., 2020; Awadallah *et al*., 2014). Ni *et al*. (2006) also discovered that Co-Mo/MgO has superior activity than Co/MgO catalyst due to the formation of Mo2C, which slows down CH4 dissociation and balances with carbon migration. According to Brachetti-sibaja *et al*. (2021), the processing temperatures and chemical treatment are the key variables determining the purity, crystallinity, thermal stability, and morphology of CNTs.

Despite the interesting contributions in producing high yield and quality CNTs, many researches simply considered either optimising the supporting material for catalyst, the process parameters of catalysts or CNTs synthesis. In order to produce high yield MWCNTs for the efficient application in pipeline corrosion protection, this work aims to investigate the effect of optimisation of the bimetallic catalyst (Co-Mo/MgO) and CNTs synthetic parameters utilising central composite and factorial design.

II. MATERIAL AND METHODS

A. *Catalyst Development*

The chemicals - 99% purity of cobalt nitrate hexahydrate ($Co(NO_3)_2 .6H_2O$) and molybdenum hexahydrate ($Mo(NO_3)_3 .6H_2O$) were obtained from Kem Light Lab. Mumbai India and MgO of 99% purity was obtained from Kermel China. In this work, Co-Mo supported on MgO was synthesised via wet impregnation method and optimised using factorial and central composite design method. About 19.4 g of $Co(NO_3)_2.6H_2O$ and 1.2 g of $Mo(NO_3)_3.6H_2O$ salts were weighed and dissolved in 50 cm^3 of distilled water. The mixture was allowed to dissolve completely and 15 g of magnesium oxide was added to it then stirred for 1 h using a magnetic stirrer at a stirring speed of 1500 rpm. The obtained slurry was dried in an oven for a period of 11 h at 115 ^oC. The dried catalyst was grinded and sieved through a 150 μm sieve aperture to obtain a uniformly sized particle specimens. The process was carried out as demonstrated by Lobiak *et al.* (2020) and Buhari *et al.* (2019). The uniformly sieved catalyst was calcined in an electric furnace at temperatures range of 500-600 ^oC and time range of 2 to 4 hrs. The obtained catalyst was characterised for the surface area, surface morphology, crystallinity and the thermal stability using TGA/DTA techniques. The percentage yield of the catalyst was calculated using the Equation 1 as follows (Buhari *et al.*, 2019);

$$\text{Catalyst Yield (\%)} = \frac{\text{Final weight of catalyst after drying(g)}}{\text{Initial weight of catalyst before drying (g)}} \times 100 \quad (1)$$

B. *Synthesis of CNTs*

The horizontal chemical vapor deposition (CVD) reactor was used to synthesise MWCNTs. 0.5 g of the produced Co-Mo/MgO catalyst was measured using a weighing balance and placed at the center of the quartz reactor. When the reaction temperature hits 700 ^oC, nitrogen gas was used to purge the reactor at a flow rate of 50 mL/min. At this temperature, the flow rate of nitrogen was raised to 200 mL/min while the flow rate of acetylene was reduced to allow the carbon nucleation process to occur for an hour-long reaction time. Immediately the reaction time was attained, the flow of acetylene was truncated and that of the nitrogen gas was reduced to 50 mL/min until the system cool to room temperature. The boat contain the produced carbon nanotubes were removed, weighed and the percentage Multi-walled carbon nanotubes synthesised was determined using Equation 2 (Awadallah *et al.,* 2014; Li *et al.,* 2020). The as-synthesised CNT were treated with 30 % wt (percentage weight) concentrated nitric acid, heated and stirred at a temperature of 50 $^oC$for 30 minutes using sonicator (SB25-12DTS model, manufactured by Ningbo HINOTEK Instrument Co, LTD) to remove residual portions of magnesium oxide and other catalysts materials including the accompanied impurities. The sample was washed with distilled water until the pH was approximately 7.0 and later dried at 100 ^oC for 8 hours. The purified sample was characterised using SAED and XRD crystallinity analysis.

$$\text{CNTs Yield (\%)} = \frac{\text{Final weight of CNTs after reaction(g)}}{\text{Initial weight of catalyst before reaction(g)}} \times 100 \quad (2)$$

C. *Optimisation of Catalyst and CNTs*

The application of MgO as bi-metallic catalyst support in the synthesis of CNTs was optimised with Factorial and central composite design (CCD) techniques using Design Expert 13.0 (Stat-Ease; Inc. Minneapolis, MN, USA) software. The effect of drying time on the Co-Mo/MgO catalyst was investigated by varying time between 9 to 12 h. The highest yield obtained from the optimisation process of catalyst synthesis was further optimised using a 2^4 factorial design to test for the effect of calcination temperature (500-600 ^oC) and time (2-4 hours) on the yield of the bi-metallic Co-Mo/MgO catalyst as carried out by Betar *et al.* (2021). From the optimisation results obtained, the catalyst with the highest specific surface area was employed for the synthesis of carbon nanotubes in a catalytic chemical vapour deposition reactor (CCVD). The CNTs production was optimised using 2^4 factorial design of experiment by considering time (45 and 60 min), temperature (700 and 800 ^oC), nitrogen and acetylene flow rate (200 and 250 mL/min) as the factors.

D. *Characterisation of Catalyst*

The characterisation was carried out to study materials' thermal stability, surface area and percentage purity using TGA 4000 (PerkinElmer). The sample was loaded into the equipment and recorded using pyris manager software. Samples were analysed in nitrogen environment at a flow rate of 20 mL/min, with pressure of 2.5 bars and heating rate of 10 ^oC/min. The analysis was then initiated after constant weight was noted using the created heating profile (temperature scan). The test results were obtained using pyris manager for proximate and compositional analysis. The particle size and the hydrodynamic diameter were determined using Zetasizer Nano S at scattering angle of 173^o operating at 25^{o}C with equilibrating time of 120 secs. 1 mg of the samples were dispersed in 10 mL of ethanol then transferred into a polystyrene cuvette using a syringe with 0.22 μm filter coupled to it. This was then placed in the sample holder of the equipment for analysis. The surface areas of the developed catalyst were determined using a BET method in Nova e-series

equipment. Samples were degassed at 250 °C for 4 hrs for moisture and removal. The degassed samples were then analysed for physisorption of the adsorbate (nitrogen) by the adsorbent in liquid nitrogen environment on the surface. The crystal phase identification of the powdered materials were performed using Bruker AXS D8 X-ray diffractometer system coupled with Cu-Kα radiation of 40 kV and a current of 40 mA. The λ for Kα was 0.1541 nm, scanning rate was 1.5 °C/min while a step width of 0.05° was used over the 2θ range value of 20 – 80.

III. RESULTS

A. Optimisation and Thermal Stability of Catalyst

The central composite design optimisation technique was used to optimise the use of MgO as a bi-metallic catalyst support in the synthesis of CNTs. As reported in Buhari et al. (2019), the optimisation results show that the effectiveness of heat and mass transfer through the heat of vaporisation is enhanced by the impact of drying temperature on the quality and yield of catalyst materials. The 10 h drying period, 120°C drying temperature, and 16 g of mass support material produced the best yield of 93.12% and this can be attributed to a strong driving force that enhanced the interaction between the metals (Co-Mo) and the support (MgO) at high drying temperatures. Hence, the outcome is consistent with Ezz *et al.* (2019) research on the production of Ni-Co-Mo/MgO as a catalyst.

1) Effect of Calcination on the Yield of Co-Mo/MgO catalyst

The outcome of the calcination of the Co-Mo/MgO catalyst is shown in Table 1. It was discovered that the catalyst yield at the highest calcination temperature of 500 °C and holding time of 2 h was 40.62%. , followed by catalyst yield at the same temperature and holding time of 35.24%. (4 h). The yield changed significantly as the temperature was raised to 600 °C, with yields of 32.80 and 28.30% for 2 and 4 hours respectively.

Table 1: Effect of Calcination on the Yield and Activity of Catalyst

Run	Time(h)	Temperature (°C)	Yield (%)	Surface area(m^2/g)	Pore volume (cc/g)	Pore size (nm)
1	2	500	40.62	247.30	0.053	3.91
2	4	500	35.24	270.38	0.072	3.51
3	2	600	32.80	305.40	0.140	3.60
4	4	600	28.30	326.35	0.157	3.46
Uncalcined				197.50	0.049	3.01

The surface area of Co-Mo/MgO catalyst analysed using the BET method under ideal conditions, was discovered to have ranges of values, depending on the holding duration. At 2 and 4 hours holding times, the BET specific surface areas of catalysts calcined at 500 °C were 247.30 and 270.38 m^2/g, respectively. The surface areas were 305.40 and 326.35 m^2/g at holding times of 2 and 4 hours, respectively, at a calcination temperature of 600 °C. The high surface areas of the samples at higher calcination temperatures and longer holding times resulted in a decrease in catalyst yield and thermal degradation of the catalyst, which suggests that cobalt (Co) and molybdenm (Mo) particles were widely dispersed in the support matrix. In comparison, the present study's findings are consistent with those of Numpilai *et al* (2017) and Panic *et al.* (2017).

2) Statistical Analysis of the developed catalyst

ANOVA was used to analyse the laboratory data of the central composite design experiment for the synthesis of catalysts, as shown in Table 2. The acquired results were best fit by the response surface cubic model. The cubic model was determined to accurately describe the experimental data based on the results shown in Table 2. Additionally, several parameters that significantly impacted the yield of the catalyst materials were discovered.

R-Squared = 0.9752, Adj R-Squared = 0.9216, and Adeq Precision = 17.054

The yield of the bi-metallic catalyst was positively impacted by such parameters as C, BC, C^2, ABC, and A^2C. The model is significant as observed from the Model F-value of 18.18. There is only a 0.09 % chance that a "Model F-Value" this large could occur due to noise. Model terms are considered significant when "Prob > F" is less than 0.0500.

In this instance, key model terms include BC, C^2, ABC, A^2C, and AB^2. Model terms are not significant if the value is higher than 0.1000. Model reduction may enhance a model if it has a lot of unnecessary terms (except those needed to maintain hierarchy). It was discovered that the Pred R-Squared was 1.1698. According to the "Lack of Fit F-value" of 3.24, the lack of fit is not noteworthy compared to pure error. A "Lack of Fit F-value this significant could arise owing to noise with a 13.16% probability. A negative "Pred R-Squared," showed the average mean is more accurate predictor of response than the current model. Signal-to-noise ratio is measured using "Adeq Precision." A ratio of at least 4 is preferred. A strong signal is indicated by the ratio of 17.054. To move around the design space, utilise this model. The p-values show how important the operating parameters are to the cubic model's estimated % catalyst yield. A p-value of 0.05 or less indicates that a factor is significant.

The final equation in terms of coded factors is shown in Eqn. 4, whereas the final equation in terms of significant factors are depicted in Eqn. 3.

$$\%\,\text{Yield} = 86.78 + 0.58A + 1.63B + 2.28C + 0.9AB + 0.12AC + 6.01BC + 0.35A^2 - 1.38B^2 - 4.55C^2 + 3.57ABC - 2.09A^2B + 4.13A^2C - 6.10AB^2 \quad (3)$$

The final equation representing significant factors is presented in Eqn. 4.

Table 2: Statistical analysis using ANOVA

Source	Sum of Square	Degree of freedom	Mean square	F-Value	P-value Prob > F
Model	1340.86	13	103.14	18.18	0.0009
A-Drying Time	1.90	1	1.90	0.34	0.5838
B-Drying temp	14.96	1	14.96	2.64	0.1556
C-Mass of support	29.34	1	29.34	5.17	0.0633
AB	7.05	1	7.05	1.24	0.3077
AC	0.11	1	0.11	0.019	0.8947
BC	289.32	1	289.32	50.98	0.0004
A^2	1.75	1	1.75	0.31	0.5987
B^2	27.60	1	27.60	4.86	0.0696
C^2	298.81	1	298.81	52.65	0.0003
ABC	102.03	1	102.03	17.98	0.0054
A^2B	14.47	1	14.47	2.55	0.1614
A^2C	56.42	1	56.42	9.94	0.0197
AB^2	123.14	1	123.14	21.70	0.0035
AC^2	0.000	0			
B^2C	0.000	0			
BC^2	0.000	0			
A^3	0.000	0			
B^3		0			
C^3		0			
Residual	34.05	6	5.67		
Lack of fit	13.40	1	13.40	3.24	0.1316
Pure Error	20.65	5	4.13		
Cor Total	1374.91	19			

$$\%\ \text{Yield} = 86.78 + 2.28C + 6.01BC - 4.55C^2 + 3.57ABC + 4.13A^2C \quad (4)$$

3) Effect of synthesis factors as surface and contour plots CCD

The effect and interaction of each factor on the yield of Co-Mo.MgO catalyst to produce MWCNT was investigated in a 3-D response surfaces. These effects were explained individually using statistical values with more evidence of how the effects occurred within the varying factors range. Figure 1A, 1B, and 1C shows the interaction between the process parameters when mass support held at 15 g, drying time held at 11 hours and temperature was held at 115 ºC are taking as actual factor respectively. The graphs suggest that the lower yield of 62.43 % and the highest yield of 89.09 % were obtained at mass support value range of 13.32-16.68 g, drying time in the range of 9.23-12.68 hours and drying temperature at the range of 115-123.41 ºC. The effect of drying time on the Co-Mo/MgO catalyst within the varying time showed that the catalyst yield increased and eventually falls at higher drying time. This could be attributed to volatile substances in the sample.

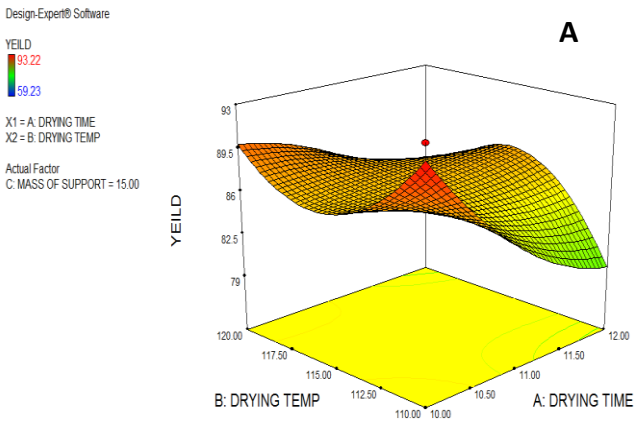

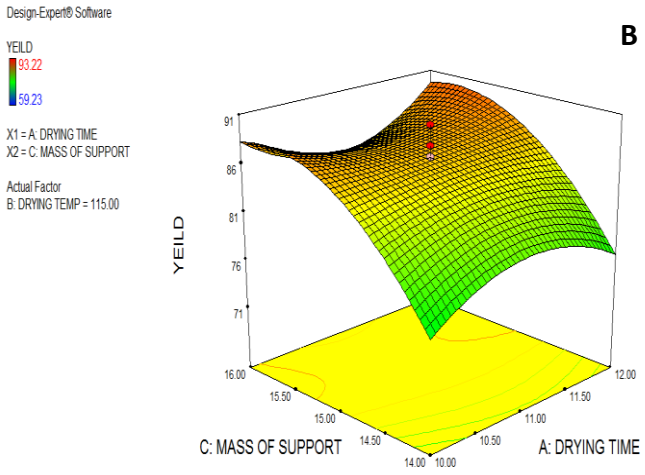

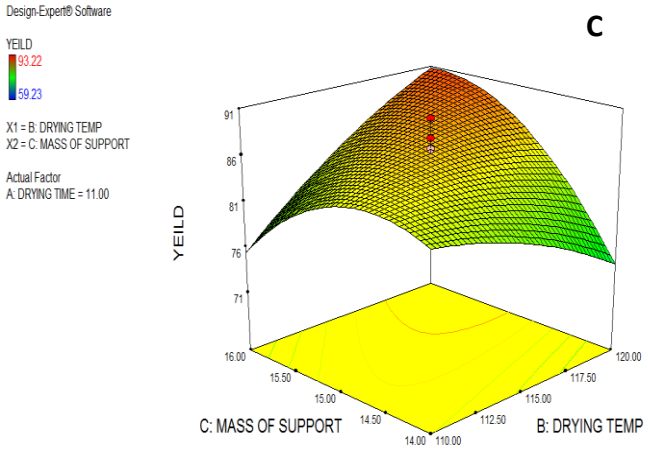

Figure 1: Response surface plot of process parameters on the yield of Co-Mo/MgO catalyst with actual factor of (A) mass of support of 15 g, (B) Drying temperature of 115 oC, (C) Drying time of 11 hours.

The catalyst yield obtained at drying time of 10 hour was found to be the highest. This could result from better metal support interactions at lower holding time leading to formation of high catalyst yield. It is shown that the catalyst yield is inversely proportional to the drying time. This finding, however, contradicted the study of Bankole *et al.* (2019) who found that the catalyst yield at high drying time led to high catalyst yield. The catalyst yield between 11 to 12 hours at drying time was lower than the catalyst yield obtained at 10 hours. This result indicates that metallic particles adsorbed via impregnation were higher than moisture diffusion leading to weight loss of sample grains observed during drying time at 10 hours than 12 hours. However, the results obtained were in line with the study of Ezz *et al.* (2019) on the production of Ni-Co-Mo/MgO as the catalyst. The result also showed that the catalyst yield increases as the drying temperature increases. The trend in the increased yield could be due to the high dispersion rate of metallic particles on the supported substrate, and the water removal rate was higher at high temperatures, which increased the catalyst yield. This can also be attributed to large driving force leading to increase in the interactive behaviour of the support (MgO) and metals (Co-Mo) at high drying temperature. The study conformed to the literature reported by Ezz *et al.* (2019). The effect of mass of support on the catalyst yield as presented in Figure 4B and 4C revealed the catalyst yield was sensitive to the MgO/Co-Mo ratios. The results indicate the adsorption rate of mass of MgO was faster, suggesting an increase in the binding site for impregnation than diffusion rate during drying process. Thus, the number of surface metal atoms increased which resulted in the increase in the active site of the catalyst and catalyst yield. This confirmed that metal oxide species effectively increase the catalyst yield. This corroborates to the finding of Aboul-Enein and Awadallah (2018) who reported that $MgMoO_x$ catalyst is effective for achieving high catalyst yield.

4) Thermal Stability of Co-Mo/MgO Catalyst

The decomposition profile for all synthesised catalyst obtained from TGA data is shown in Figure 2. The PerkinElmer TGA machine with Pyris manager software retrieved the moisture content, onset temperature, degradation profile, peak degradation temperature, and percentage weight loss at 800 oC. Table 3 displays the outcomes of the parameters that were extracted. By turning the nitrates in the samples into oxides, the final heat treatment by calcination eliminated the nitrates and any remaining moisture. According to Couteau et al. (2003), precise particle size control is necessary for best performance because it may alter the rate and selectivity. In order to minimise particle sizes, increase surface area, and ultimately increase catalytic activity, calcinations were used. Additionally, Shanmugam et al. (2020) noted that the calcination temperature significantly impacted the catalyst activity.

The proximate analysis of produced bi-metallic catalyst obtained from the TGA/DTA thermograph, is shown in Table 3. The percentage degradation and loss for the uncalcined catalyst sample were found to be 24.74 and 60.64%, respectively. The loss of water (departure of the hydration water), coordinated water, and water molecules from -OH groups can all be linked to the exothermic and endothermic processes seen in the DTA data for all samples.

The removal of water is the cause of this endothermic reaction. A few peaks were visible on the DTG curves, which are connected to the regular departure of the hydration water, coordinated water, and structural water molecules from -OH groups. The uncalcined catalyst sample contained the highest percentage composition of degraded material. This can be due to the loose water content in the sample of the uncalcined catalyst. Thus, the catalyst produced at 600 ^oC for 4 hours shows fewer of these qualities. Due to the catalyst material's prolonged exposure to a very high temperature of 600 ^oC during the calcination process, the percentage of volatile content degradation and the percentage loss decreased. The loss of the physiosorbed and chemisorbed water molecules, which Aliyu et al. (2017) also observed, was thought to cause the weight loss at this temperature. The research conducted by Ramasubramanian *et al.* (2020) is supported by the fact that the catalyst was dry at the temperature before the drop in moisture. The volatile content may be caused by a Co-Mo-containing molecule in the catalyst mixture.

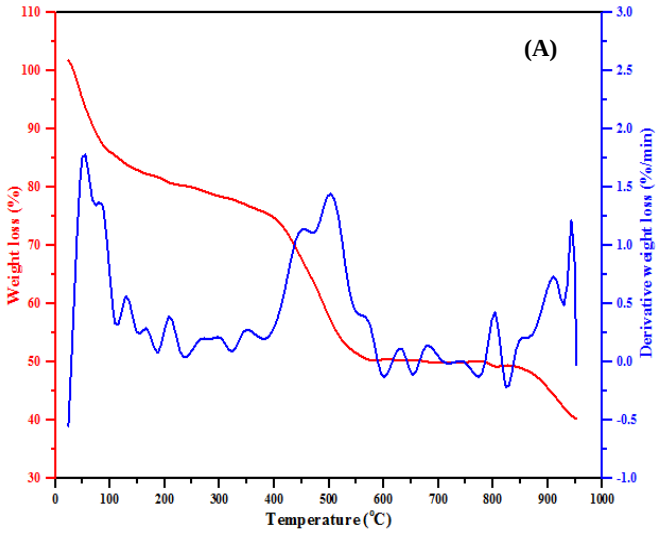

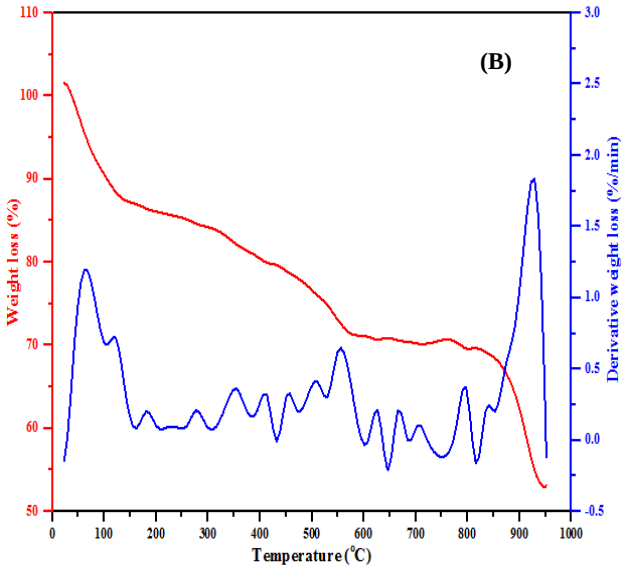

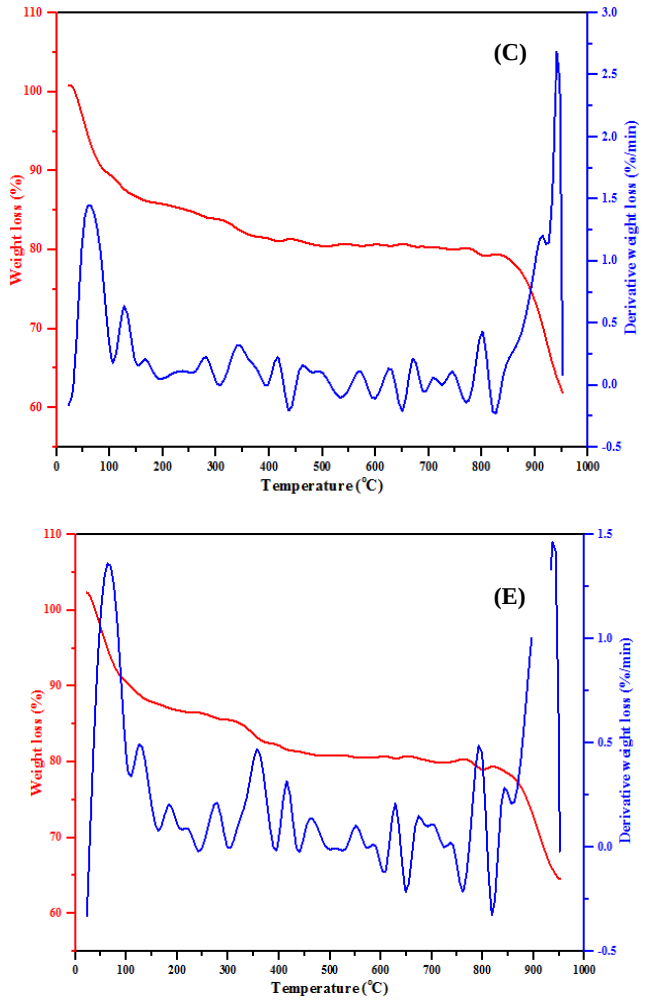

Figure 2: TGA/DTA thermograph of (A) uncalcined (B) calcined at 2h at 500 ºC (C) calcined at 4h at 500ºC (D) calcined at 2h at 600 ºC and (E) calcined at 4h at 600ºC of Co-Mo/MgO bi-metallic catalyst.

reported on a related investigation and found that catalyst weight loss at temperatures above 700 ºC showed excellent thermostability. Thus, it is evident that the preparation of the catalyst is greatly influenced by greater calcination temperatures.

B. Optimisation and Crystallinity properties of CNT

1) Effect of process parameter on the yield of CNTs

The Synthesis of CNTs by CVD technique was optimised using 2^4 factorial design of experiment. The highest specific surface area catalyst was employed in the CNT synthesis process. The maximum yield of 1.59 g, according to the results shown in Table 4, was obtained under the ideal conditions of synthesis time of 45 min, temperature of 700 ºC, nitrogen flow rate of 250 mL/min, and acetylene flow rate of 250 mL/min. The findings suggest that the process parameter influences the CNT yield.

Table 3: Proximate composition of Co-Mo/MgO bi-metallic catalyst

Catalyst	Onset Temp (ºC)	Peak degradation Temp (ºC)	% degradation	% loss at 800ºC
Uncalcined catalyst	321.98	497.94	24.74	60.64
Catalyst at 2h at 500ºC	339.19	416.81	9.87	23.91
Catalyst at 4h at 500ºC	374.81	432.72	7.01	20.87
Catalyst at 2h at 600ºC	357.47	396.41	4.88	17.67
Catalyst at 4h at 600ºC	398.21	437.03	4.11	12.09

The degradation temperatures of the uncalcined catalyst and the catalyst calcined at 500 ºC and 600 ºC for 2 h and 4 h, respectively, were 321.98 ºC and 357.47 ºC. However, the uncalcined catalyst was shown to have a lower onset temperature than other calcined catalysts, which may be attributed to the material's unbound water and volatile chemicals, which are either practically absent or present in much lower amounts in other calcined catalyst formulations. With a degradation temperature of 357.47 ºC, it exhibited a unique material degree of crystallinity and textural characteristics. This might also result from the prolonged high-temperature calcination process, which can remove the unbound water content and transform the catalyst into a more crystal-like state with enhanced thermal properties. Zhao *et al.* (2016)

2) Effect of Growth temperature on yield

The yield of carbon nanotubes formed at growth temperature is shown in Table 4 using the CVD technique. Interestingly, large yield was achieved at 700 ºC. However, the carbon nanotubes decrease by increasing the temperature to 800 ºC. The increase in carbon nanotubes yield at temperature of 700 ºC could be due to the increase in the diffusion rate and solubility of catalyst particles. At this point, the metal atoms become mobile and the larger size of particle aggregate is achieved, which increase the nucleation, yield and growth of carbon nanotubes (Ezz *et al.*, 2019). The high yield could also be ascribed to high dispersion of active cobalt oxide species by the interaction with MgO and MoO_3 (Aboul-Enein and Awadallah, 2018). This study is in agreement with Ezz *et al.* (2019) finding

Table 4: 2^4 Factorial Design of experiment for CNT synthesis

Runs	Block	Factor 1 A:Time (T)	Factor 2 B:Temperature (C)	Factor 3 C:Nitrogen flow (mL/min)	Factor 4 D:Acetylene flow (mL/min)	Response Weight (g)
1	Block 1	60.00	700.00	250.00	200.00	1.14
2	Block 1	60.00	800.00	200.00	250.00	0.92
3	Block 1	60.00	700.00	200.00	200.00	0.87
4	Block 1	45.00	800.00	200.00	250.00	0.94
5	Block 1	60.00	700.00	200.00	250.00	0.94
6	Block 1	60.00	800.00	250.00	250.00	0.96
7	Block 1	60.00	800.00	250.00	200.00	0.99
8	Block 1	45.00	700.00	200.00	250.00	1.04
9	Block 1	45.00	800.00	200.00	200.00	1.09
10	Block 1	60.00	800.00	200.00	200.00	1.55
11	Block 1	60.00	700.00	250.00	250.00	0.66
12	Block 1	45.00	800.00	250.00	250.00	0.99
13	Block 1	45.00	700.00	200.00	200.00	0.74
14	Block 1	45.00	800.00	250.00	200.00	0.98
15	Block 1	45.00	700.00	250.00	250.00	1.59
16	Block 1	45.00	700.00	250.00	200.00	1.17

that reported the increase in carbon yield can be achieved with increasing growth temperature.

Similar trend was observed under constant growing time of 60 min at the growing temperature of 800 ºC as presented in Table 4. This result shows that all the carbon nanotubes produced is inversely proportional to the growth temperature indicating encapsulation of carbon deposit onto the Co-Mo metallic particles and partial decomposition of the carbon source at 800 ºC. Furthermore, the low yield of CNTs could be influenced by agglomeration and deactivation of metallic particles between Co-Mo and MgO. This study has proven that higher temperature may not be favourable for high quality and quantity CNTs. This finding corresponds to the study of Oyewemi *et al.* (2019).

3) Effect of growth time on yield

The yield of CNTs under the influence of growth time at temperature 700 ºC is presented in Table 4. The yield increases as the growing time increases as it is represented with weight responses in Table 4. This may be related to the formation of Co-Mo alloy phase during the interaction between Co-Mo/MgO and acetylene. The high yield at relatively 45 min is attributed to the less accumulation of catalyst and agglomeration of metallic particles. In this study, it is obvious that the formation of CNTs was attained at high growth time. This could be associated with the stability between the acetylene gas and the surface sites of the synthesised catalyst particles (Aliyu *et al.,* 2017). This also corresponds to the report of Abdulkareem *et al.* (2017) and Ezz *et al.* (2019), who synthesised CNTs from Fe-Co-Ni/$CaCO_3$ and Fe-Ni-Co-Mo/MgO Catalyst, respectively. Comparison between the obtained yield with other previous literature via bimetallic and multimetallic catalyst under similar conditions (Abdulkareem *et al.,* 2017; Aliyu *et al.,* 2017) showed that the catalyst used in this present study is more efficient for yielding quality CNTs.

4) Effect of acetylene flow rate and nitrogen flow rate

The effects of acetylene flow and nitrogen flow on the percentage production of carbon nanotubes in a CVD reactor are examined in Table 5. The results show that the maximum catalyst yield was found at an acetylene flow rate of 250 mL/min and a nitrogen flow rate of 100 mL/min. In contrast, the amount of CNTs that were deposited decreased as acetylene flow rate increased to 250 mL/min from the nitrogen flow rate of 150 mL/min. The presence of decomposable carbon from acetylene at high flow rates and the lower flow rates of nitrogen gas, the carrier gas during the nucleation process, may cause this behaviour of substantial carbon nanotube yield. While the interaction between the fraction of acetylene flow rate and nitrogen flow rate can be attributed to the low CNT synthesis yield.

Additionally, this can be explained by suppressing acetylene gas carrier decomposition, and the blockage of catalyst active sites enhanced the nitrogen gas. Therefore, high yield carbon nanotube synthesis is advantageous at lower nitrogen flow rates. Dai et al. (2014) reported that the dilution of the acetylene by adding nitrogen gas decreased the quantity of C2H2 molecules that interacted on the surface of the Co catalyst utilised. Using H2 and N2 as carrier gases, Khorrami and Lotfi (2016) discovered that the amounts of deposited carbon reduced with increasing flow rate.

Table 5: Effect of CNT operating parameters

S/N	Acetylene flow (mL/min)	Nitrogen flow (mL/min)	% yield
1	200	100	70.67
2	200	150	62.43
3	250	100	89.09
4	250	150	76.78

5) HR-TEM micrograph of the developed carbon nanotubes

The internal structure of the developed MWCNTs with the highest and lowest yields were examined via HR-TEM techniques shown in Figure 3. The HRTEM of the Co-Mo/MgO catalyst as shown in Figure 3 gave some particles which appeared as dark spots with light support material. Figure 3 (a) shows the minute quantity of blackish-like materials linked to the possible presence of catalyst constituents and amorphous carbon materials formed during the synthesis process. This observation implies that the higher the acetylene flow rate over a catalyst material during a carbon nanotubes nucleation process, the lower the impurities. The bamboo-like structure of

CNTs as seen in Figure 3, is governed by three steps namely; the degradation/transformation of carbon from acetylene into carbon atom, the diffusion and precipitation of carbon tom on the surface of catalyst. The formation steps accompanied the formation of catalyst particles as hollow structures and growth of a bamboo-like structure in the CNTs. The diameter of the produced carbon nanotubes was observed to depend on the flow rate of acetylene and the nitrogen gas. The diameters of the CNTs as revealed in Figure 3 (b) was found to be 45.03 nm at 250 mL/min and 100 mL/min for both acetylene and nitrogen flow rate, respectively. The diameter of the carbon nanotubes produced at lower acetylene flow of 200 mL/min and constant nitrogen flow rate resulted in the production of higher diameter carbon nanotubes. This shows that the produced carbon nanotubes is a multi-walled carbon nanotubes with several tubes walls.

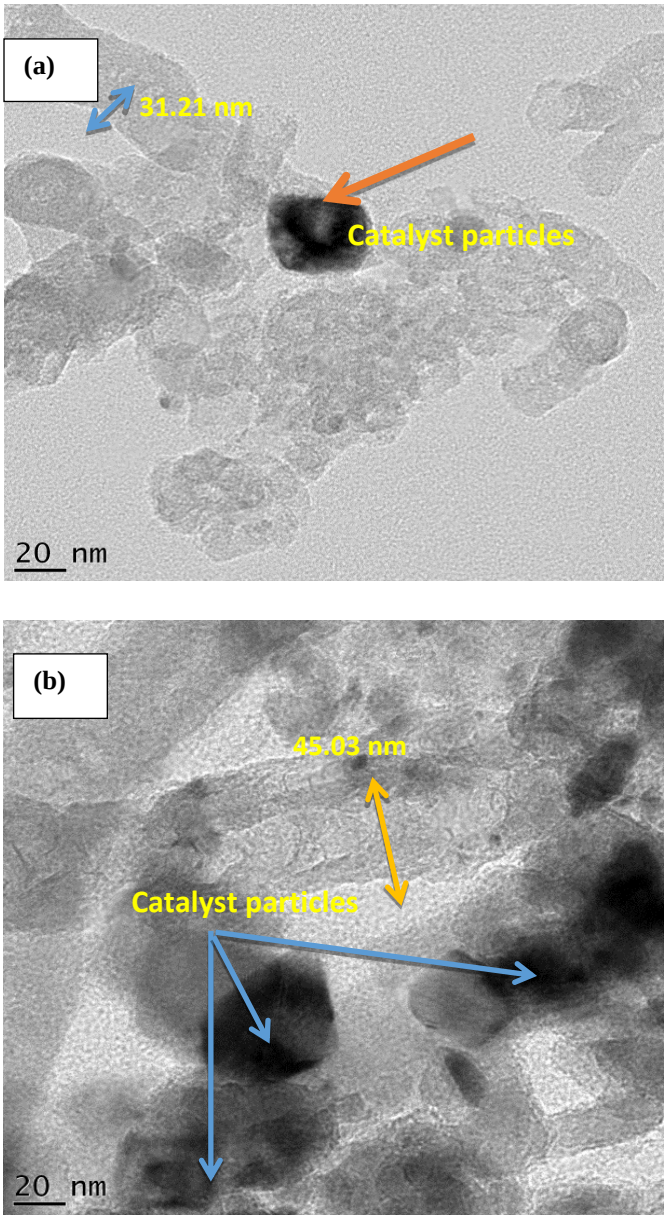

Figure 3: HR-TEM micrographs of (a) highest yield CNTs and (b) lowest yield CNTs.

6) XRD micrograph of the developed CNTs

The crystallinity of the synthesised CNTs was determined using XRD technique; the analysis result is presented in Figure 4. The result presented shows two noticeable peaks at the diffraction angle of 25.34 and 45.21 for both the low and high yield CNTs. These peaks represent the formation of graphitised carbon, which indicates CNTs formation. The peak at 25.34° with (002) plane which represents the graphitic peak emerged as a result of the tubular pattern of the carbon which is consistent with Neupane *et al.* (2014) finding. The two prominent peaks for high yield CNTs as shown in Figure 4, designating the first on the left, have a higher intensity with less width than the second peak at the right. The peak 45.21° (100) plane at the right is usually considered crystalline or amorphous. The reduction in intensity due to the increase in width refers to the amorphous crystal form of carbon nanotubes.

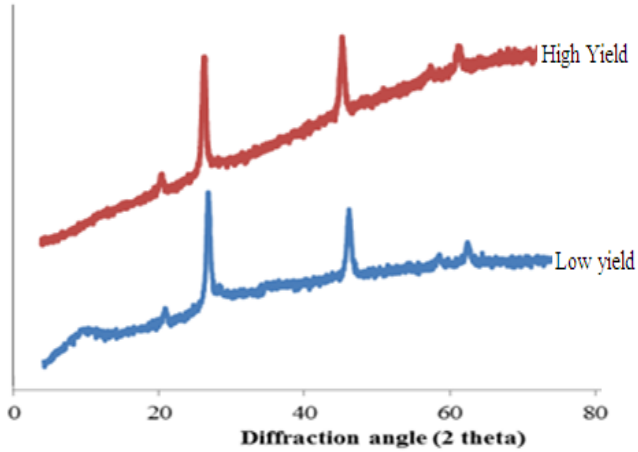

Figure 4: XRD spectral of the developed CNTs.

7) SAED micrograph of the developed CNTs

Figure 5 (a-b) shows the result of the selected area electron diffraction spectroscopy (SAED) of the developed CNTs. The SAED results show the graphitised nature of the developed CNTs.

From Figure 5 (a-b), the SAED pattern of both CNTs produced at varied acetylene flow rate has no variation in their crystal lattice. However, the ring nature of the CNTs produced contains disjointed rings indicating the presence of encapsulated catalyst crystals. The growth of CNTs with the Co-Mo/MgO catalyst had CNT structure consisting of concentric graphene pattern as shown in selective area electron diffraction (SAED). The SAED patterns of CNTs synthesised shows a high fine dispersion of amorphous nanostructure as seen in Figure 5a. The selected area electron diffraction (SAED) patterns of the CNTs (Figure 5b) also revealed the presence of circular bright spots. The concentric circle with (200) plane could be ascribed as an increase in the carbon inter-layer structure of graphite (Neupane *et al.*, 2014; brachetti-sibaja *et al.*, 2021). The diffraction rings pattern is similar to the diffraction peaks in the XRD pattern rings which correspond to the (002), and (100) miller indices, respectively which is consistent with the X-ray diffraction micrograph.

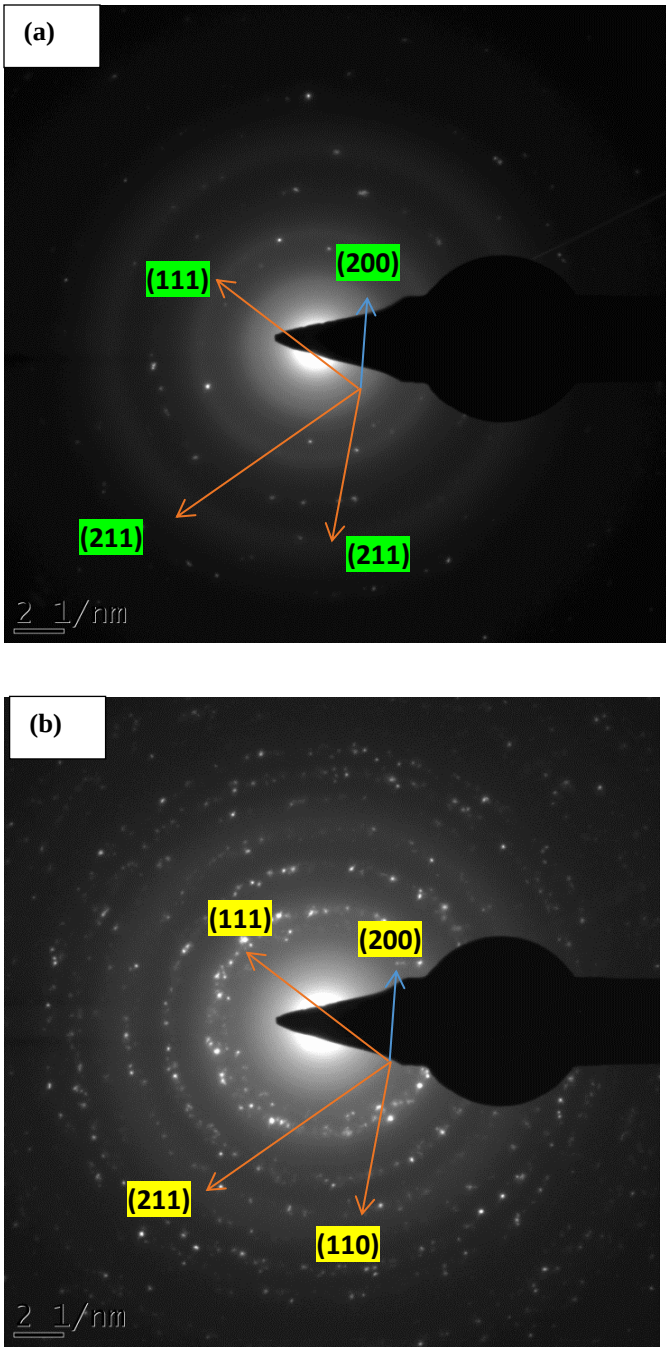

Figure 5: SAED Pattern of the developed (a) highest yield CNTs and (b) lowest yield CNTs.

IV. CONCLUSION

The Co-Mo/MgO catalyst with optimum yield of 40.62%, surface area of 247.30 m^2/g at 500ºC drying temperature, mass support of 16 g and 10 h dry time were obtained. The lowest yield of 62.43 % and the highest yield of (89.09 %) were obtained at mass support value range of 13.32-16.68 g, drying time in the range of 9.23-12.68 hours and drying temperature at the range of 115-123.41 ºC. The calcination temperature and holding time severely influence the catalyst yield regarding specific area, pore size and volume. The catalyst calcined for a period of 4 h at 600 ºC had the highest degradation temperature of 357.47 ºC . The XRD and SAED reveal the growth of CNTs with the Co-Mo/MgO catalyst, which consists of a concentric graphene pattern and the diameters of the CNTs were found to be 31.21 nm at the optimal value of 250 mL/min and 100 mL/min for both acetylene and nitrogen flow rate, respectively. During this stage, the reaction from the oxidised metal catalyst occurs during the reduction of cobalt oxide and molybdenum oxide to carbide when the hydrocarbon precursor is decomposed.

AUTHOR CONTRIBUTIONS

S. Buahri: Conceptualization, Methodology, Data curation, Validation, Writing – original draft. **A. S. Abdulrahaman:** Supervision, Funding acquisition, Writing – review & editing. **S.A. Lawal:** Resources**,** Writing – review & editing. **A.S. Abdulkareem:** Supervision, Investigation. **R. A. Muriana:** Writing – review & editing. **O. T. Jimoh:** Investigation, Formal analysis; Writing – review & editing. **H. K. Ibrahim:** Formal analysis; Writing – original draft.

ACKNOWLEDEGMENTS

The authors wish to appreciate the Tertiary Education Trust Fund (TETFund) Nigeria for supporting this research with grant (TETFund/FUTMINNA/2019/B7/13).

REFERENCES

Abdulkareem, A. S.; I. Kariim; M. T. Bankole; J. O. Tijani; T. F. Abodunrin and S. C. Olu. (2017). Synthesis and Characterisation of Tri-metallic Fe–Co–Ni Catalyst Supported on $CaCO_3$ for Multi-Walled Carbon Nanotubes Growth via Chemical Vapor Deposition Technique. Arabian Journal for Science and Engineering, 42(10), 4365–4381. doi:10.1007/s13369-017-2478-2

Aliyu, A.; A. S. Abdulkareem; A. S. Kovo; O. K. Abubakre; J. O. Tijani and I. Kariim. (2017). Synthesise multi-walled carbon nanotubes via catalytic chemical vapour deposition method on Fe-Ni bimetallic catalyst supported on kaolin. Carbon Letters (Carbon Lett.), 21, 33-50.

Awadallah, A. E.; A. A. Aboul-Enein and Aboul-Gheit, A. K. (2014). Impact of group VI metals addition to Co/MgO catalyst for non-oxidative decomposition of methane into COx-free hydrogen and carbon nanotubes. Fuel, 129, 27–36. doi:10.1016/j.fuel.2014.03.038.

Betar, B.O.; M. A. Alsaadi; Z. Z. Chowdhury; M. K. Aroua; F. S. Mjalli and M. M. Niazi. (2021). High Yield Super-Hydrophobic Carbon Nanomaterials Using Cobalt/Iron Co-Catalyst Impregnated on Powder Activated Carbon. Processes, 9, 134. https://doi.org/10.3390/ pr9010134.

Brachetti-Sibaja, S. B.; D. Palma-Ramírez; A. M. Torres-Huerta; M. A. omínguez-Crespo; H. J. Dorantes-Rosales; A. E. Rodríguez-Salazar and E. Ramírez-Meneses (2021). CVD Conditions for MWCNTs Production and Their Effects on the Optical and Electrical Properties of PPy/MWCNTs, PANI/MWCNTs Nanocomposites by In Situ Electropolymerization. Polymers, 13, 351. https:// doi.org/10.3390/polym13030351.

Buhari, S. A.; A. S. Abdulrahman; A. S. Abdulkareem; S. A. Lawal and I. B. Akintunde. (2019). Synthesis of Carbon Nanotubes using Catalytic Chemical

Vapour Decomposition of Acetylene over Co-Mo bimetallic Catalyst supported on Magnesia, Nigerian Journal of Engineering and Applied Sciences Vol. 6 No. 1, pp. 46-57.

Camilli, L.; M. Scarselli; S. Del Gobbo; P. Castrucci; P. Nanni; E. Gautron; S. Lefrant and M. De Crescenzi. (2011). The synthesis and characterisation of carbon nanotubes grown by chemical vapor deposition using a stainless steel catalyst. Carbon, 49(10), 3307–3315. doi:10.1016/j.carbon.2011.04.014.

Couteau, E.; K. Hernadi; J. W. Seo; J. W. Thiên-Nga; C. Mikó; R. Gaál and L. Forró. (2003). CVD synthesis of high-purity multiwalled carbon nanotubes using $CaCO_3$ catalyst support for large-scale production. Chemical Physics Letters, 378(1-2), 9–17. doi:10.1016/s0009-2614(03)01218-1

Dai, Y.; S. Liu and N. Zheng. (2014). C2H2 Treatment as a Facile Method to Boost the Catalysis of Pd Nanoparticulate Catalysts. Journal of the American Chemical Society, 136(15), 5583–5586. doi:10.1021/ja501530n

Ezz, A. A.; M. M. Kamel and G. R. Saad. (2019). Synthesis and characterisation of nanocarbon having different morphological structures by chemical vapor deposition over Fe-Ni-Co-Mo/MgO catalyst. Journal of Saudi Chemical Society, 23(6), 666–677. doi:10.1016/j.jscs.2018.11.004.

Kariim, I.; A. S. Abdulkareem; O. K. Abubakre; I. A. Mohammed; M. T. Bankole and O. T. Jimoh. (2015). Studies on the suitability of alumina as bimetallic catalyst support for MWCNTs growth in a CVD reactor. 1st International Engineering Conference (IEC) Minna, Nigeria. 296-305.

Khorrami, S. A. and Lotfi, R. (2016). Influence of carrier gas flow rate on carbon nanotubes growth by TCVD with Cu catalyst. Journal of Saudi Chemical Society, 20(4), 432–436. doi:10.1016/j.jscs.2013.04.004

Kim, P. and Lee, C. (2018). The Reduction Temperature Effect of Fe–Co/MgO Catalyst on Characteristics of Multi-Walled Carbon Nanotubes. Catalysts, 8(9), 361. doi:10.3390/catal8090361

Li, D.; L. Tong and B. Gao. (2020). Synthesis of Multiwalled Carbon Nanotubes on Stainless Steel by Atmospheric Pressure Microwave Plasma Chemical Vapor Deposition. Applied Sciences, 10(13), 4468. doi:10.3390/app10134468

Li, K.; H. Zhang; Y. Zheng; G. Yuan; Q. Jia and S. Zhang. (2020). Catalytic Preparation of Carbon Nanotubes from Waste Polyethylene Using FeNi Bimetallic Nanocatalyst. Nanomaterials, 10(8), 1517. doi:10.3390/nano10081517.

Lobiak, E. V.; V. R. Kuznetsova; E. Flahaut; A. V. Okotrub and L. G. Bulusheva. (2020). Effect of Co-Mo catalyst preparation and CH4/H2 flow on carbon nanotube synthesis, Fullerenes Nanotubes and Carbon Nanostructures, 28 (9). 1-9. ISSN 1536-383X

Neupane, S.; Y. Yang; W. Li and Y. Gao. (2014). Synthesis and enhanced electron field emission of vertically aligned carbon nanotubes grown on stainless steel substrate, Journal of Nanoscience Letters, 4:14, pp. 1-8.

Ni, L.; K. J. Kuroda; L. P. Zhou; T. Kizuka; K. Ohta and K. Matsuishi. (2006). Kinetic study of carbon nanotube synthesis over Mo/Co/MgO catalysts. Carbon, 44: 22. 65–72.

Numpilai, T.; T. Witoon; N. Chanlek; W. Limphirat; G. Bonura; M. Chareonpanich and J. Limtrakul. (2017). Structure–activity relationships of Fe-Co/K-Al_2O_3 catalysts calcined at different temperatures for CO_2 hydrogenation to light olefins. Applied Catalysis A: General, 547, 219-229.

Oyewemi, A.; A. S. Abdulkareem; J. O. Tijani; M. T. Bankole; O. K. Abubakre; O. K. Afolabi and W. D. Roos. (2019). Controlled Syntheses of Multi-walled Carbon Nanotubes from Bimetallic Fe–Co Catalyst Supported on Kaolin by Chemical Vapour Deposition Method. Arabian Journal for Science and Engineering. doi:10.1007/s13369-018-03696-4

Panic, S.; B. Bajac; S. Rakić; Á. Kukovecz; Z. Kónya; V. Srdić and G. Boskovic. (2017). Molybdenum anchoring effect in Fe–Mo/MgO catalyst for multiwalled carbon nanotube synthesis. Reaction Kinetics, Mechanisms and Catalysis, 122(2), 775–791. doi:10.1007/s11144-017-1291-y.

Ramasubramanian, V.; H. Ramsurn and G. L. Price. (2020). Hydrogen production by catalytic decomposition of methane over Fe based bi-metallic catalysts supported on CeO_2–ZrO_2. International Journal of Hydrogen Energy, 45, 12026-12036.

Ryu, H.; B. K. Singh and K. S. Bartwal (2008). Synthesis and Optimisation of MWCNTs on Co-Ni/MgO by Thermal CVD. Advances in Condensed Matter Physics, 2008, 1–6. doi:10.1155/2008/971457

Shanmugam, K.; J. Manivannan and M. Manjuladevi. (2020). Stupendous Nanomaterials: Carbon Nanotubes Synthesis, Characterisation, and Applications. Nanomaterials - Toxicity, Human Health and Environment. doi:10.5772/intechopen.90318

Thapa, A.; S. Neupane; R. Guo; K. L. Jungjohann; D. Pete and W. Li. (2018). Direct growth of vertically aligned carbon nanotubes on stainless steel by plasma enhanced chemical vapor deposition. Diamond and Related Materials, 90, 144–153. doi:10.1016/j.diamond.2018.10.012

Tijani, J. O.; U. A. Aminu; M. T. Bankole; M. M. Ndamitso and A. S. Abdulkareem. (2020). Adsorptive and Photocatalytic Properties of Green Synthesized ZnO and ZnO/NiFe2O4
Nanocomposites for Tannery Wastewater Treatment, Nigerian Journal of Technological Development (NJTD), Vol. 17, No.4, pp. 312-322, doi: http://dx.doi.org/10.4314/njtd.v17i4.10.

Zhao, Q.; J. Yao; L. Shi and X. Wang (2016). Effect of calcination temperature on structure, composition and properties of $S_2O_8^{2-}/ZrO_2$ and its catalytic performance for removal of trace olefins from aromatics. RSC Advances, 6(87), 84553-84561.